IOSR Journal Of Applied Physics (IOSR-JAP)
e-ISSN: 2278-4861.Volume 18, Issue 2 Ser. 1 (Mar – Apr 2026), PP 55-62
www.Iosrjournals.Org

Structural, Thermal and Photoluminescence Analysis of Pr^{3+} Doped Borophosphate Glasses for the Visible Light Emitting Diodes Applications

S.L.Meena
Ceramic Laboratory, Department of physics, Jai Narain Vyas University, Jodhpur 342001(Raj.) Ind

Abstract
Zinc lithium alumino sodalime potassiumniobate borophosphate glasses containing Pr^{3+} in (20-x):P_2O_5: 10ZnO: 10Li_2O: 10Al_2O_3: 10Na_2O: 10CaO: 10K_2O: 10Nb_2O_5:10B_2O_3:xPr_2O_3 (where x=1, 1.5,2 mol %) have been prepared by melt-quenching method. The amorphous nature of the glasses was confirmed by x-ray diffraction studies. Optical absorption, Excitation spectra and fluorescence spectra were recorded at room temperature for all glass samples. Judd-Ofelt intensity parameters Ω_λ (λ=2, 4, 6) are evaluated from the intensities of various absorption bands of optical absorption spectra. Using these intensity parameters various radiative properties like spontaneous emission probability, branching ratio, radiative life time and stimulated emission cross–section of various emission lines have been evaluated. Large thermal stability shows that the prepared glass samples is useful thermionic applications.
Keywords: *ZLASLPNBP Glasses, Optical Properties, Judd-Ofelt Theory, Thermal Properties.*

Date of Submission: 16-03-2026 Date of Acceptance: 26-03-2026

I. Introduction

Glass ceramics have been widely reported and are generally obtained by using treatment techniques to control crystallization of glass samples. Glass ceramics possess better mechanical performance and higher chemical and thermal stability than the parent glass-ceramics [1-5]. Among different glasses phosphate glasses have unique properties. They have high transparency, good mechanical and chemical stability [6-8].Phosphate glasses are extremely attractive materials for physical, optical, linear and nonlinear properties such as high refractive index, low phonon energy, high dielectric constant, low melting temperature, high thermal stability and good solubility [9-12].The addition of heavy metal oxide to borophosphate glasses increase the quantum efficiency and decrease the phonon energy.The addition of ZnO increases the refractive index while decreases the optical energy band gap. The addition of network modifier (NWF) Li_2O is to improve both electrical and mechanical properties of such glasses. Pr^{3+} doped glasses are very important because of the possibility of their application in optoelectronic device fields, such as lasers, fiber optics and solar cells [13-15].

In this work, the spectral and thermal properties of Pr^{3+} -doped (20-x):P_2O_5: 10ZnO: 10Li_2O: 10Al_2O_3: 10Na_2O: 10CaO: 10K_2O: 10Nb_2O_5:10B_2O_3:xPr_2O_3 (where x=1, 1.5,2 mol %) glasses were investigated. The DTA thermogram, absorption, Excitation and fluorescence spectra of Pr^{3+} of the glasses were investigated. The J-O intensity parameters render significant information regarding local structure and bonding in the vicinity of rare- earth ions.

II. Experimental Techniques

Preparation of glasses

The following Pr^{3+} doped Zinc lithium alumino sodalime potassiumniobate borophosphate glass samples (20-x):P_2O_5: 10ZnO: 10Li_2O: 10Al_2O_3: 10Na_2O: 10CaO: 10K_2O: 10Nb_2O_5:10B_2O_3:xPr_2O_3 (where x=1, 1.5.2) have been prepared by melt-quenching method. Analytical reagent grade chemical used in the present study consist of P_2O_5, ZnO, Li_2O,Al_2O_3,Na_2O,CaO,K_2O,Nb_2O_5, $B_2O_3$and Pr_2O_3. All weighed chemicals were powdered by using an Agate pestle mortar and mixed thoroughly before each batch (10g) was melted in alumina crucibles in silicon carbide based an electrical furnace.

Silicon Carbide Muffle furnace was heated to working temperature of 1055^0C, for preparation of Zinc lithium alumino sodalime potassiumniobate borophosphate glasses, for two hours to ensure the melt to be free from gases. The melt was stirred several times to ensure homogeneity. For quenching, the melt was quickly poured on the steel plate & was immediately inserted in the muffle furnace for annealing. The steel plate was preheated to100^0C.While pouring; the temperature of crucible was also maintained to prevent crystallization. And annealed at temperature of 350^0C for 2h to remove thermal strains and stresses. Every time fine powder of cerium oxide was used for polishing the samples. The glass samples so prepared were of good optical quality

and were transparent. The chemical compositions of the glasses with the name of samples are summarized in Table 1

Table 1 Chemical composition of the glasses

Sample	Glass composition (mol %)
ZLASLPNBP (UD)	$20P_2O_5$: 10ZnO: $10Li_2O$: $10Al_2O_3$: $10Na_2O$: 10CaO: $10K_2O$: $10Nb_2O_5$:$10B_2O_3$
ZLASLPNBP PR (1.0)	$19P_2O_5$: 10ZnO: $10Li_2O$: $10Al_2O_3$: $10Na_2O$: 10CaO: $10K_2O$: $10Nb_2O_5$:$10B_2O_3$:$1Pr_2O_3$
ZLASLPNBPPR(1.5)	$18.5P_2O_5$:10ZnO: $10Li_2O$: $10Al_2O_3$: $10Na_2O$: 10CaO: $10K_2O$: $10Nb_2O_5$:$10B_2O_3$:$1.5Pr_2O_3$
ZLASLPNBP PR (2.0)	$18P_2O_5$: 10ZnO: $10Li_2O$: $10Al_2O_3$: $10Na_2O$: 10CaO: $10K_2O$: $10Nb_2O_5$:$10B_2O_3$:$2Pr_2O_3$

ZLASLPNBP (UD)—Represents undoped Zinc lithium alumino sodalime potassiumniobate borophosphate glass specimen.
ZLASLPNBP (PR) -Represents Pr^{3+} Zinc lithium alumino sodalime potassiumniobate borophosphate glass specimens.

III. Theory

3.1 Oscillator Strength

The intensity of spectral lines are expressed in terms of oscillator strengths using the relation [16].

$$f_{expt.} = 4.318 \times 10^{-9} \int \varepsilon(\nu)\, d\nu \qquad (1)$$

Where, ε (ν) is molar absorption coefficient at a given energy ν (cm^{-1}), to be evaluated from Beer–Lambert law. Under Gaussian Approximation, using Beer–Lambert law, the observed oscillator strengths of the absorption bands have been experimentally calculated, using the modified relation [17].

$$P_m = 4.6 \times 10^{-9} \times \frac{1}{cl} \log \frac{I_0}{I} \times \Delta\upsilon_{1/2} \qquad (2)$$

where c is the molar concentration of the absorbing ion per unit volume, I is the optical path length, $\log I_0/I$ is absorbtivity or optical density and $\Delta\upsilon_{1/2}$ is half band width.

3.2. Judd-Ofelt Intensity Parameters

According to Judd [18] and Ofelt [19] theory, independently derived expression for the oscillator strength of the induced forced electric dipole transitions between an initial J manifold $|4f^N (S, L) J\rangle$ level and the terminal J' manifold $|4f^N (S',L') J'\rangle$ is given by:

$$\frac{8\Pi^2 mc\bar{\upsilon}}{3h(2J+1)} \frac{1}{n}\left[\frac{(n^2+2)^2}{9}\right] \times S(J, J') \qquad (3)$$

where, the line strength S (J, J') is given by the equation

$$S(J, J') = e^2 \sum \Omega_\lambda \langle 4f^N (S, L)\, J \| U^{(\lambda)} \| 4f^N (S', L')\, J' \rangle^2 \qquad (4)$$

$\lambda = 2, 4, 6$

In the above equation m is the mass of an electron, c is the velocity of light, ν is the wave number of the transition, h is Planck's constant, n is the refractive index, J and J' are the total angular momentum of the initial and final level respectively, Ω_λ (λ = 2, 4 and 6) are known as Judd-Ofelt intensity parameters.

3.3.Radiative Properties

The Ω_λ parameters obtained using the absorption spectral results have been used to predict radiative properties such as spontaneous emission probability (A) and radiative life time (τ_R), and laser parameters like fluorescence branching ratio (β_R) and stimulated emission cross section (σ_p).

The spontaneous emission probability from initial manifold $|4f^N (S', L') J'\rangle$ to a final manifold $|4f^N (S, L) J\rangle$ is given by:

$$A[(S', L') J'; (S, L) J] = \frac{64\pi^4 \nu^3}{3h(2J'+1)} \left[\frac{n(n^2+2)^2}{9}\right] \times S(J', J) \qquad (5)$$

Where, $S(J', J) = e^2 [\Omega_2 \| U^{(2)} \|^2 + \Omega_4 \| U^{(4)} \|^2 + \Omega_6 \| U^{(6)} \|^2]$

The fluorescence branching ratio for the transitions originating from a specific initial manifold $|4f^N (S', L') J'>$ to a final many fold $|4f^N (S, L) J >$ is given by

$$\beta[(S', L') J'; (S, L) J] = \sum_{S L J} \frac{A[(S' L') J' (S L)]}{A[(S' L') J' (S L)]} \quad (6)$$

where, the sum is over all terminal manifolds.

The radiative life time is given by

$$\tau_{rad} = \sum_{S L J} A[(S', L') J'; (S,L)] = A^{-1}_{Total} \quad (7)$$

where, the sum is over all possible terminal manifolds. The stimulated emission cross -section for a transition from an initial manifold $|4f^N (S', L') J'>$ to a final manifold $|4f^N (S, L) J >|$ is expressed as

$$\sigma_p(\lambda_p) = \left[\frac{\lambda_p^4}{8\pi c n^2 \Delta\lambda_{eff}}\right] \times A\left[(S', L') J'; (S, L) J\right] \quad (8)$$

where, λ_p the peak fluorescence wavelength of the emission band and $\Delta\lambda_{eff}$ is the effective fluorescence line width.

3.4 Nephelauxetic Ratio (β) and Bonding Parameter ($b^{1/2}$)

The nature of the R-O bond is known by the Nephelauxetic Ratio (β') and Bonding Parameters ($b^{1/2}$), which are computed by using following formulae [20, 21]. The Nephelauxetic Ratio is given by

$$\beta' = \frac{\nu_g}{\nu_a} \quad (9)$$

where, ν_a and ν_g refer to the energies of the corresponding transition in the glass and free ion, respectively. The values of bonding parameter $b^{1/2}$ are given by

$$b^{1/2} = \left[\frac{1-\beta'}{2}\right]^{1/2} \quad (10)$$

IV. Result and Discussion

4.1 XRD Measurement

Figure 1 presents the XRD pattern of the samples containing show no sharp Bragg's peak, but only a broad diffuse hump around low angle region. This is the clear indication of amorphous nature with in the resolution limit of XRD instrument.

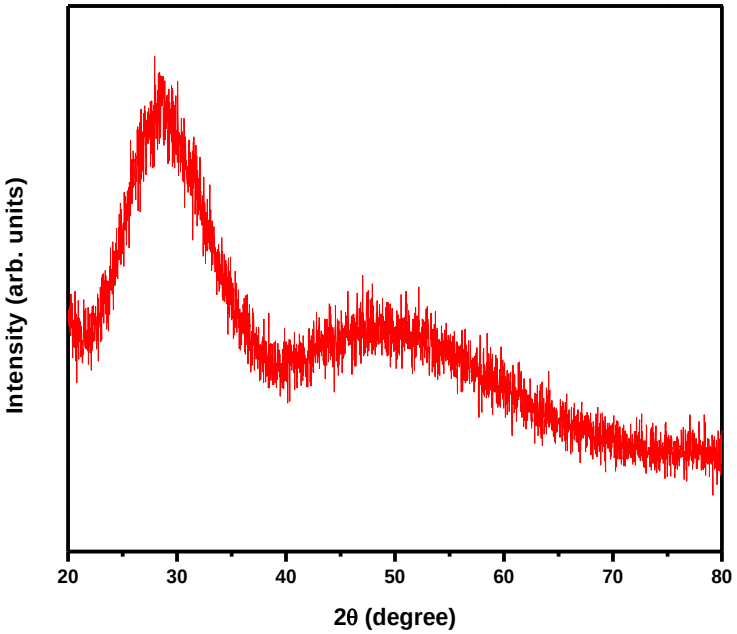

Fig.1: X-ray diffraction pattern of ZLASLPNBP PR (1.0) glass.

4.2 Thermal Property

Differential thermal analysis checks the heat absorbed by glass samples during heating or cooling. Fig. 2 depicts the DTA thermogram of powdered ZLASLPNBP sample. The glass transition temperature (T_g), onset crystallization temperature (T_c), crystallization temperature (T_p), melting temperature(T_m), thermal stability

(T_s),Balaji Parameter (B_P), Hurbe's criterion (H_R) and reduced glass transition temperature (T_{rg}) were calculated. Shankar's parameter also calculated by using eq. (12). All the determined thermal parameters are given in table 2.

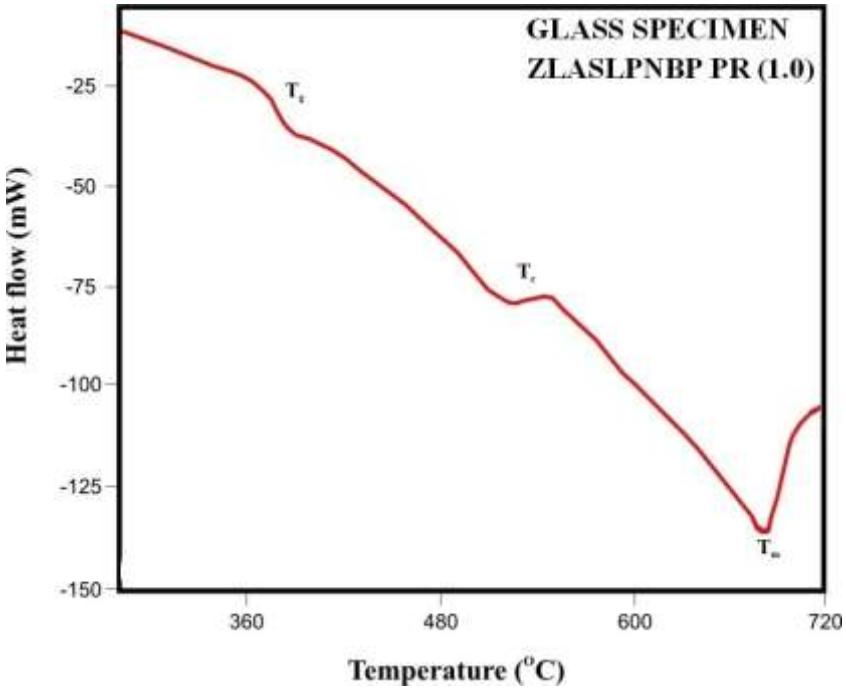

Fig.2: DTA curve of YZLASLPNBP PR (1.0) glass.

Table 2. Thermal parameters determined from the DTA traces of ZLASLPNBP PR glasses.

Sample Name	T_g(°C)	T_c(°C)	T_p(°C)	T_m(°C)	T_s(°C)	B_P(°C)	H_R(°C)	K_S(°C)	T_{rg}(°C)
ZLASLPNBP PR (1.0)	375	509	548	685	134	3.436	0.222	34.429	0.547
ZLASLPNBP PR (1.5)	380	510	551	687	130	3.171	0.232	33.493	0.553
ZLASLPNBP PR (2.0)	385	512	555	692	127	2.953	0.239	33.035	0.556

The thermal stability of the glass samples can be calculated by difference between onset crystallization temperature and transition temperature [22].

Thermal Stability (T_s)= T_c-T_g (11)

Balaji Parameter can be calculated using [23].

Balaji Parameter (B_P) = $[(T_c-T_g)/(T_p-T_c)]$ (12)

Hruby's criterion is calculated using the Hurby's relation [23].

Hruby'scriterion(H_R)=$[(T_p-T_c)/(T_m-T_c)]$ (13)

Reduced glass transition temperature is given as [23].

Reduced glass transition temperature (T_{rg}) =T_g/T_m (14)

Thermal Parameter is given as [23].
$K_S= [(T_m-T_c)\ (T_c-T_g)/T_m]$ (15)

4.3 Absorption spectra

The absorption spectra of ZLASLPNBP PR (1.0) glass, consists of absorption bands corresponding to the absorptions from the ground state $^3H_4$ of Pr^{3+} ions. Eight absorption bands have been observed from the ground state $^3H_4$ to excited states $^3F_2$, $^3F_3$, $^3F_4$, $^1G_4$, $^1D_2$, $^3P_0$, $^3P_1$ and $^3P_2$ for Pr^{3+} doped ZLASLPNBP PR(1.0) glass.

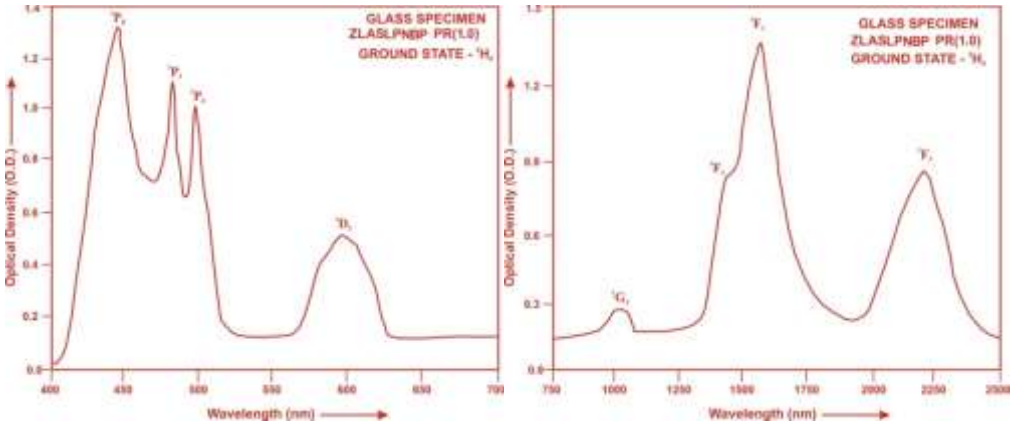

Fig.3: Absorption spectra of ZLASLPNBP PR (1.0) glass.

The experimental and calculated oscillator strengths for Pr^{3+} ions Zinc lithium alumino sodalime potassiumniobate borophosphate glasses are given in **Table 3**

Table 3. Measured and calculated oscillator strength ($P^m \times 10^{+6}$) of Pr^{3+} ions in ZLASLPNBP glasses.

Energy level $^3H_4$	Glass ZLASLPNBP PR(1.0)		Glass ZLASLPNBP PR(1.5)		Glass ZLASLPNBP PR(2.0)	
	$P_{exp.}$	$P_{cal.}$	$P_{exp.}$	$P_{cal.}$	$P_{exp.}$	$P_{cal.}$
$^3F_2$	4.63	3.81	3.65	2.92	2.64	2.15
$^3F_3$	6.43	5.55	5.23	4.35	4.74	3.98
$^3F_4$	4.46	3.57	3.39	2.82	2.45	2.47
$^1G_4$	0.43	0.29	0.39	0.23	0.25	0.21
$^1D_2$	2.39	0.99	1.98	0.78	1.37	0.71
$^3P_0$	4.67	1.00	3.68	0.73	2.68	1.05
$^3P_1$	4.86	1.96	3.84	1.47	2.90	1.80
$^3P_2$	12.33	3.31	11.64	2.61	10.53	2.36
R.m.s.deviation	3.6626		3.5156		2.9986	

The various energy interaction parameters like Slater-Condon parameters F_k (k=2, 4, 6), Lande′ parameter ξ_{4f} and Racah parameters E^k (k=1, 2, 3) have been computed The ratio of Racah parameters E^1/E^3 and E^2/E^3 are about 9.789 and 0.0484 respectively. Computed values of Slater-Condon, Lande′, Racah, nephelauexetic ratio and bonding parameter for Pr^{3+} doped ZLASLPNBP glass specimens are given in **Table 4**.

Table4. Computed values of Slater-Condon, Lande′, Racah, nephelauexetic ratio and bonding parameter for Pr^{3+} doped ZLASLPNBP glass specimens.

Parameter	Free ion	ZLASLPNBP PR(1.0)	ZLASLPNBP PR(1.5)	ZLASLPNBP PR(2.0)
$F_2(cm^{-1})$	322.09	300.03	300.01	300.01
$F_4(cm^{-1})$	44.46	44.28	44.27	44.26
$F_6(cm^{-1})$	4.867	4.414	4.412	4.412
$\xi_{4f}(cm^{-1})$	741.00	858.27	858.41	858.59
$E^1(cm^{-1})$	4728.92	4451.74	4450.98	4450.88
$E^2(cm^{-1})$	24.75	22.01	22.01	22.01
$E^3(cm^{-1})$	478.10	454.73	454.74	454.69
F_4/F_2	0.13804	0.14757	0.14755	0.14752
F_6/F_2	0.01511	0.01471	0.01470	0.01471
E^1/E^3	9.8911	9.7899	9.7881	9.7888
E^2/E^3	0.0518	0.0484	0.0484	0.0484
β'		0.8888	0.8887	0.8887
$b^{1/2}$		0.2357	0.2359	0.2359

Judd-Ofelt intensity parameters Ω_λ (λ = 2, 4 and 6) were calculated by using the fitting approximation of the experimental oscillator strengths .

The values of Judd-Ofelt intensity parameters are given in **Table 5**.

Table 5. Judd-Ofelt intensity parameters for Pr^{3+} doped ZLASLPNBP glass specimens.

Glass Specimen	$\Omega_2(pm^2)$	$\Omega_4(pm^2)$	$\Omega_6(pm^2)$	Ω_4/Ω_6	Ref.
ZLASLPNBP PR(1.0)	3.369	1.520	5.496	0.277	P.W.
ZLASLPNBP PR(1.5)	2.582	1.114	4.346	0.256	P.W.
ZLASLPNBP PR(2.0)	1.430	1.598	3.768	0.424	P.W.
BAPBP (PR)	2.290	2.278	2.742	0.831	[24]
ZLASVBB (ER)	0.7825	0.2697	0.8768	0.308	[25]

4.4 Excitation Spectrum

Excitation spectra of ZLASLPNBP PR (1.0) glass recorded at the emission wavelength 395 nm is depicted as figure 4. The excitation spectra consists of three peaks corresponding to the transitions from the ground state $^3H_4$ to the various excited states $^3P_2$, $^3P_1$ and $^3P_0$ at the wavelengths of 448, 465 and 486 nm respectively. Among these, a prominent excitation band at 448 nm has been selected for the measurement of emission spectrum of Pr^{3+} glass.

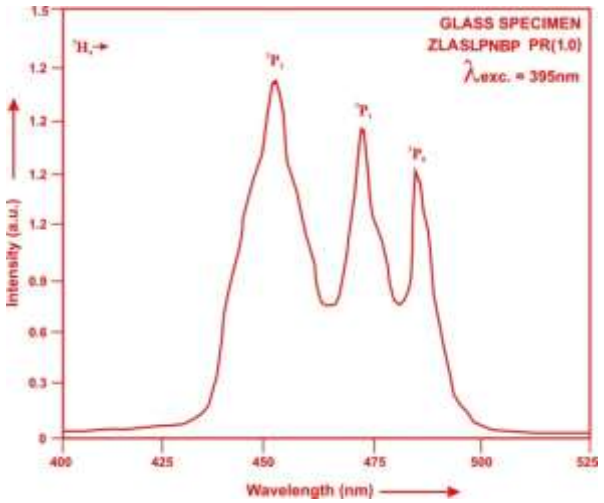

Fig.4: Excitation Spectrum of ZLASLPNBP PR (1.0) glass.

4.5 Fluorescence Spectrum

The fluorescence spectrum of Pr^{3+}doped in zinc lithium alumino sodalime potassiumniobate borophosphate glass is shown in Figure 5. There are eleven broad bands ($^3P_0 \rightarrow {}^3H_4$), ($^3P_0 \rightarrow {}^3H_5$), ($^1D_2 \rightarrow {}^3H_4$), ($^3P_0 \rightarrow {}^3H_6$), ($^3P_0 \rightarrow {}^3F_2$), ($^3P_1 \rightarrow {}^3F_3$), ($^1D_2 \rightarrow {}^3H_5$), ($^3P_0 \rightarrow {}^3F_4$), ($^1G_4 \rightarrow {}^3H_5$), ($^1G_4 \rightarrow {}^3H_6$) and ($^1G_4 \rightarrow$ ($^3F_4$, $^3F_2$))and respectively for glass specimens.

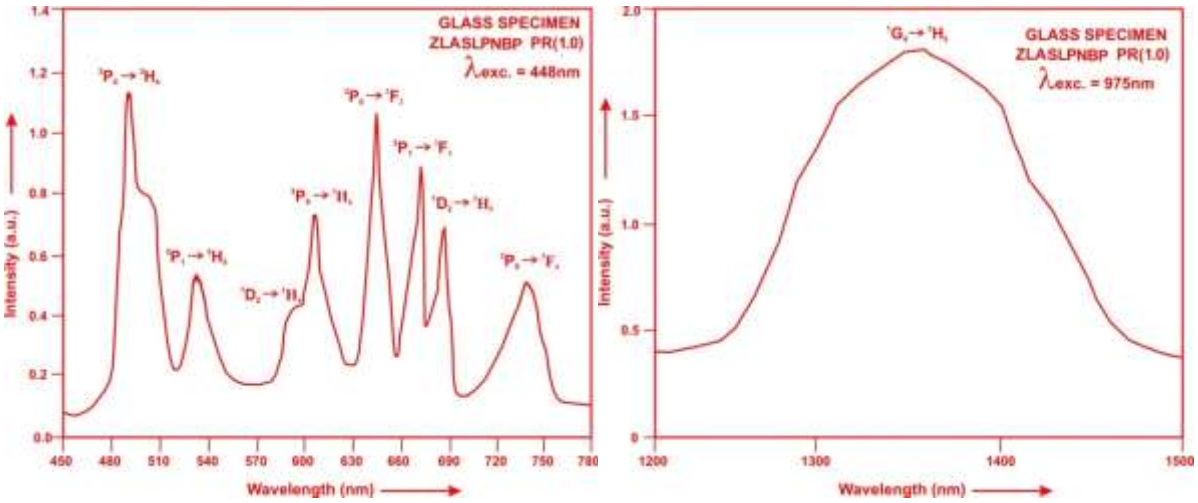

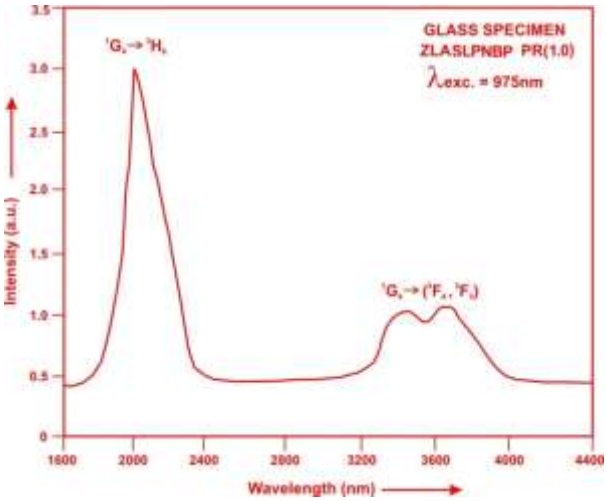

Fig.5: Fluorescence spectrum of ZLASLPNBP PR (1.0) glass.

Table 6. Emission peak wave lengths (λ_p), radiative transition probability (A_{rad}), branching ratio (β_R), stimulated emission crosssection (σ_p), and radiative life time (τ) for various transitions in Pr^{3+} doped ZLASLPNBP glasses.

Transition		ZLASLPNBP PR (1.0)				ZLASLPNBP PR (1.5)				ZLASLPNBP PR(2.0)			
	λ_{max} (nm)	$A_{rad}(s^{-1})$	β	σ_p (10^{-20} cm^2)	τ_R(μs)	$A_{rad}(s^{-1})$	β	σ_p(10^{-20} cm^2)	τ_R (μs)	$A_{rad}(s^{-1})$	β	σ_p (10^{-20} cm^2)	τ_R (10^{-20} cm^2)
$^3P_0 \rightarrow {}^3H_4$	485	783.61	0.0829	0.271		575.45	0.0796	0.204		827.11	0.1384	0.306	
$^3P_1 \rightarrow {}^3H_5$	529	1725.13	0.1826	0.354		1319.89	0.1825	0.276		1485.06	0.2485	0.315	
$^1D_2 \rightarrow {}^3H_4$	599	483.68	0.0512	0.200		380.65	0.0526	0.159		344.82	0.0577	0.147	
$^3P_0 \rightarrow {}^3H_6$	602	434.73	0.0460	0.240		344.45	0.0476	0.195		299.24	0.0501	0.172	
$^3P_0 \rightarrow {}^3F_2$	645	2304.14	0.2438	2.202	105.82	1769.42	0.2447	1.750	138.27	981.92	0.1643	1.007	167.34
$^3P_1 \rightarrow {}^3F_3$	676	3177.47	0.3363	1.802		2425.75	0.3354	1.390		1622.57	0.2715	0.945	
$^1D_2 \rightarrow {}^3H_5$	685	4.45	0.0005	0.0049		3.376	0.0005	0.0038		3.99	0.0007	0.005	
$^3P_0 \rightarrow {}^3F_4$	730	144.75	0.0153	0.114		106.30	0.0147	0.0843		152.79	0.0256	0.122	
$^1G_4 \rightarrow {}^3H_5$	1350	234.06	0.0248	0.828		184.44	0.0255	0.656		162.57	0.0272	0.580	
$^1G_4 \rightarrow {}^3H_6$	2025	139.03	0.0147	5.166		108.09	0.0149	4.068		86.02	0.0144	3.265	
$^1G_4 \rightarrow (^3F_4, {}^3F_2)$	3555	18.59	0.0020	3.475		14.20	0.0020	2.670		9.87	0.0017	1.868	

V. Conclusion

In the present study, the glass samples of composition (20-x):P_2O_5: 10ZnO: 10Li_2O: 10Al_2O_3: 10Na_3O: 10CaO: 10K_2O: 10Nb_2O_5:10B_2O_5:xPr_2O_3 (where x =1, 1.5, 2 mol %) have been prepared by melt-quenching method. The stimulated emission cross-section (σ_p) has highest value for the transition ($^1G_4 \rightarrow {}^3H_6$) in all the glass specimen doped with Pr^{3+}ion. This shows that ($^1G_4 \rightarrow {}^3H_6$) transition is most probable transition and it useful for laser action. The thermal stability parameter for prepared glass samples are very large therefor, these samples can be good materials for fiber fabrication.

References

[1]. Meena,S.L.(2025).Spectral, Thermal and Raman Analysis of Ho3+ doped Borophosphate glasses with large Balaji Parameter, IOSR Appl.Phys.17,24-31.
[2]. Meena,S.L.(2025).Spectral and Photoluminescence Properties of Nd3+ doped Borotellurite Glasses for 1.08μm photonic devices, IOSR Appl.Phys.17,28-33.
[3]. Bondzior,B.,Lisiecki,R.(2024).Excellent Color Purity and Luminescence Thermometry Performance in Germanate Tellurite Glass Doped with Eu3+,Appl.Sci.14,1-15.
[4]. B.Naziha,Lezid,M.,Goumeidane,F.,Legouera,M.,Prasad,P.S.,Rao,P.V.(2023).Judd-Ofelt Analysis and Spectroscopy study of tellurite glasses doped with Rare-Earth(Nd3+,Dy3+ and Er3+)Materials,16,1-19.
[5]. Farag,M.A.,Lbrahim,A.,Hassaan,M.Y.,Ramadan,R.M.(2022).Enhancement of structural and optical properties of transparent sodium zinc phosphate glass-ceramic nano composite,J.Aust.Ceram.58:653-661.
[6]. Singh,H.,Bhatia,V.,Kumar,D.,Singh,T.S.,Singh,D.,Singh,S.P.(2022).Influence of Er3+ on structural and optical properties of borophosphate glasses,Appl.Phys.429,1-13.
[7]. Marzouk,M.A.,Ali,I.S.(2024).Enhancing the luminescent properties of strontium phosphate glass via controlled crystallization and rare earth dopant,35:1767,1-18.

[8]. Meena, S.L. (2022). Spectral and FTIR Analysis of Dy3+ ions doped Zinc Lithium Cadmium Magnesium Borophosphate Glasses, Int. J. For Res. In App. Sci. and Eng. Technology, 10(8), 55-61.
[9]. Sayed,M.A.,Ali,M.A.,El-Rehim,A.F.,Wahab,E.A.A.,Shaaban,Kh.s.,J.of Elect Materias,11664-021-0892-9.
[10]. ElMaaref,A.A.,Badr,S.,Shaaban,Kh.S.,Wahab,E.A.A.,Elokr,M.M.(2019).Optical properties and radiative rate of Nd3+ doped zinc-sodium phosphate glasses, J.Rare Earths,37,253-259.
[11]. Guidini,P.,Galleani,G.,Faria,W.,Silva,I.D.A.,Eckert,H.,Camargo,A.S.S.de,J.Non-Cryst.Solids,529,119752,1-10.
[12]. Damodaraiah, S., Prasad, V. R., Babu, S. and Ratnakaram, Y. C. (2017). Structural and luminescence properties of Dy3+ doped bismuth phosphate glasses for greenish yellow light applications. Optical Materials, 67, 14-24.
[13]. Sun,Y.Yu,F.,Liao,M.,Wang,Xin,Li,Y.,Hu,L.,Knight,J.(2020).Emission properties of Pr3+ doped aluminosilicate glasses at visible wavelengths,J.Lumines.220,117013,1-6.
[14]. Shen,Y.Z.X.,Zhou,M.,Su,X.,Li,J.,Yang,G.,Shao,H.,Zhou,Y.(2019).Ultra-broadband 1.0μm band emission spectroscopy in Pr3+/Nd3+/Yb3+ tri-doped tellurite glass, Spect.Acta Part A: Mol.andBio.Spect.222,117178.
[15]. Ding,D.,Gao,J.,Zhang,S.Duo,L.(2020).The photoluminescence properties of Pr3+-Yb3+ co-doped gallo-germanate glasses and glass ceramic as energy converter,J.Lumin.226,117512.
[16]. Meena,S.L.(2025).Spectral and Raman Analysis of Tb3+ doped Yttrium Zinc Lithium Ceasium Barium Borate Glasses,IOSR Appl.Phys.17,41-47.
[17]. Meena,S.L.(2021).Spectral and Raman Analysis of Sm3+ doped in Zinc Lithium Sodalime Alumino Silicate Glasses,Int.J.Eng.Sci.Inven.10,28-33.
[18]. Judd, B.R. (1962). Optical Absorption Intensities of Rare Earth Ions. Physical Review, 127, 750.
[19]. Ofelt, G.S. (1962). Intensities of Crystal Spectra of Rare Earth Ions. The J. Chem. Phys., 37, 511.
[20]. Kashif,I.Ratep,A.(2023).Luminescence in Er3+ co-doped bismuth germinate glass-ceramics for blue and green emitting applications,J.Korean Ceram.Soc.60,511-526.
[21]. Meena,S.L.(2021).Spectral and Raman Analysis of Er3+ doped Zinc Lithium Antimony Sodalime Tellurite Glasses,Int.J.Eng.Sci.Inv.10,09-15.
[22]. Rojas,S.S.,Souza,J.E.,Yukimitu,Hernades,A.C.(2014).Structural,thermal and optical properties of CaO and CaLiBO glasses doped with Eu3+,J.Non-Cryst.Solids,398-399,57-61.
[23]. Meena,S.L.(2025).Spectral,Thermal and Raman Analysis of Dy3+ doped Borosilicate Glasses with Large Thermal Stability Parameter,Int.J.Eng.Sci.Inv.14,11-18.
[24]. Zhang,L.,Xia,Yu,Shen,X.,Wei,W.(2019).Concentration dependence of visible luminescence from Pr3+ doped phosphate glasses, Spect.Acta Part A: Mol.and Bio.Spect.206,454-459.
[25]. Meena,S.L.(2020).Spectroscopic Properties of Er3+ doped Zinc Lithium Arsenic Strontium Vanadium Bismuth Borate Glasses,IOSR,Appl.Phys.12,05-10.